THE JOURNAL OF BIOLOGICAL CHEMISTRY
Vol. 277, No. 40, Issue of October 4, pp. 37619–37623, 2002
Printed in U.S.A.

Iron Incorporation into *Escherichia coli* Dps Gives Rise to a Ferritin-like Microcrystalline Core*

Received for publication, June 21, 2002, and in revised form, August 2, 2002
Published, JBC Papers in Press, August 5, 2002, DOI 10.1074/jbc.M206186200

Andrea Ilari‡, Pierpaolo Ceci‡, Davide Ferrari§, Gian Luigi Rossi§, and Emilia Chiancone‡¶

From the ‡C.N.R., Centro di Studio sulla Biologia Molecolare and Dipartimento di Scienze Biochimiche, "A. Rossi Fanelli," Università di Roma "La Sapienza," 00185 Roma, Italy and the §Dipartimento di Biochimica e Biologia Molecolare, Università degli Studi di Parma, 43100 Parma, Italy

***Escherichia coli* Dps belongs to a family of bacterial stress-induced proteins to protect DNA from oxidative damage. It shares with *Listeria innocua* ferritin several structural features, such as the quaternary assemblage and the presence of an unusual ferroxidase center. Indeed, it was recently recognized to be able to oxidize and incorporate iron. Since ferritins are endowed with the unique capacity to direct iron deposition toward formation of a microcrystalline core, the structure of iron deposited in the *E. coli* Dps cavity was studied. Polarized single crystal absorption microspectrophotometry of iron-loaded Dps shows that iron ions are oriented. The spectral properties in the high spin $3d^5$ configuration point to a crystal form with tetrahedral symmetry where the tetrahedron center is occupied by iron ions and the vertices by oxygen. Crystals of iron-loaded Dps also show that, as in mammalian ferritins, iron does not remain bound to the site after oxidation has taken place. The kinetics of the iron reduction/release process induced by dithionite were measured in the crystal and in solution. The reaction appears to have two phases, with $t_{1/2}$ of a few seconds and several minutes at neutral pH values, as in canonical ferritins. This behavior is attributed to a similar composition of the iron core.**

The recent work on *Listeria innocua* ferritin has disclosed that the functions of iron oxidation, uptake, and storage in a bioavailable form are not associated uniquely to the highly conserved structure of typical ferritins (1–3). This is an assemblage of 24 identical or very similar subunits that are folded in a four-helix bundle and form a spherical shell characterized by 432 symmetry. The protein is tailored to carry out efficiently the different steps leading to iron storage. Thus, the negatively charged channels along the 3-fold symmetry axes allow entry of Fe(II), the ferroxidase sites located within the four-helix bundle of the so-called H-type subunits catalyze iron oxidation by molecular oxygen, and the negatively charged internal cavity favors deposition of an oxyhydroxide core containing up to 4500 iron atoms (4–6). A notable feature of the apoferritin moiety is its capacity to direct iron deposition toward formation of a microcrystalline structure whose characteristics have been elucidated by Mössbauer spectroscopy and x-ray diffraction studies on horse spleen and human ferritin. Basically, the microcrystalline core contains oxygen atoms packed 3 Å apart (7) and iron atoms placed in spaces between oxygen layers so that they can be coordinated either octahedrically or tetrahedrically (8).

In *L. innocua* ferritin, iron oxidation and incorporation are associated to a protein that bears a high structural similarity to the Dps proteins (DNA-binding proteins from starved cells), a family of stress-induced polypeptides that bind DNA without apparent sequence specificity and prevent its cleavage by oxidative damage (3). The subunits of *L. innocua* ferritin as those of the Dps proteins do not contain the canonical ferroxidase site residues; they fold into a four-helix bundle, but assemble into a dodecameric structure with 23 symmetry (9, 10). It follows that the structural elements associated with the iron oxidation-uptake process have distinct features relative to classical ferritins. The most remarkable difference concerns the ferroxidase site, which is placed at the interface between 2-fold symmetry-related subunits such that both subunits furnish the iron-coordinating ligands. On the other hand, access of Fe(II) to the ferroxidase site and deposition of Fe(III) take place similarly to classical ferritins, since both the channels along the 3-fold symmetry axes and the surface of the internal cavity are lined with negatively charged amino acid residues. In the Dps proteins, most of the residues that coordinate the metal in the *Listeria* ferroxidase site are conserved and are part of the so-called "DNA-binding signature." Therefore, it was suggested that all the members of the Dps family are endowed with iron uptake properties (9). Indeed, *Escherichia coli* Dps, the family prototype, and the *Helicobacter pylori* neutrophil-activating protein were shown to incorporate iron (11, 12). Moreover, the study of *E. coli* Dps disclosed an unforeseen ability to use hydrogen peroxide rather than oxygen in iron oxidation and suggested a slow clearance of Fe(III) from the ferroxidase sites.

It is not known whether the ferritin-like properties of *E. coli* Dps extend to the formation of a microcrystalline core. This point is addressed in the present work. Iron-loaded *E. coli* Dps crystals have been studied by polarized single crystal absorption microspectrophotometry (Ref. 13 and references therein). This technique is particularly apt to assess the nature of the iron core, since Fe(III) in the high spin $3d^5$ configuration gives rise to different absorption bands in the visible region depending on whether it is coordinated tetrahedrally or octahedrally. In the case of a microcrystalline core, the different projections of the transition moments of the various chromophores on the crystal axes would lead to polarized absorption spectra distinct from the solution (isotropic) spectrum. A second point that has been addressed concerns more specifically the ferroxidase site. Crystals of iron-loaded Dps have been used to establish whether iron remains bound to the site after oxidation has taken place. This aspect is relevant not only in connection with

* This work was supported by grants "Agenzia 2000" from Consiglio Nazionale delle Ricerche (to A. I.) and "Biologia Strutturale e Dinamica Molecolare di Proteine Redox" (to G. L. R. and E. C.) and local funds from Ministero Istruzione Università e Ricerca (to E. C.). The costs of publication of this article were defrayed in part by the payment of page charges. This article must therefore be hereby marked "*advertisement*" in accordance with 18 U.S.C. Section 1734 solely to indicate this fact.

¶ To whom correspondence should be addressed: C.N.R., Centro di Studio sulla Biologia Molecolare and Dipartimento di Scienze Biochimiche, "A. Rossi Fanelli," Università di Roma "La Sapienza," 00185 Roma, Italy. E-mail: emilia.chiancone@uniroma1.it.

the slow clearance of Fe(III) reported by Zhao *et al.* (11), but also in more general terms, since direct observations of iron bound to the ferritin ferroxidase sites have been made only on *Listeria* ferritin and *E. coli* ferritin FTNa (9).

The present results show that *E. coli* Dps directs iron deposition toward formation of a microcrystalline iron core, where iron is coordinated tetrahedrically, and furnish additional evidence for the ferritin-like function of this protein. In iron-loaded Dps crystals, two water molecules replace the metal ions at the ferroxidase site, indicating that iron, once oxidized, leaves the site, a typical property of mammalian ferritins.

EXPERIMENTAL PROCEDURES

Protein Purification and Crystallization—The protein was purified from the *E. coli* Dps expression strain ZK1100, kindly provided by Dr. S. E. Finkel, as described in Ref. 14 with the modifications given in Ref. 11. Dps thus purified usually contains only a few iron atoms per dodecamer. Therefore, it was incubated in the presence of air with ferrous sulfate in an amount corresponding to 400 iron atoms/dodecamer. The iron oxidation/incorporation process was followed spectrophotometrically at 310 nm (15). The amount of iron incorporated in the protein shell was found to correspond to 255 ± 42 iron atoms/dodecamer as shown by analytical ultracentrifugation (11) and by evaluation of the Fe(II) 2,2′-bipyridyl complex, resulting upon denaturation of the protein and reduction of the iron with thioglycollate (16).

Dps containing 255 ± 42 iron atoms/dodecamer was crystallized by the hanging drop vapor-diffusion technique as described by Grant *et al.* (10). The protein solution (2 μl) was mixed with an equal volume of reservoir solution containing 0.1 M Tris-HCl, pH = 7.8, 1.4–1.7 M sodium formiate, and 9–12% PEG[1] 8000, as the crystal-stabilizing agent. The crystals thus obtained will be referred to as iron-loaded.

X-ray Data Collection and Structure Refinement—Different data sets were collected using 0.5 oscillation frames on the x-ray beamline at the ELETTRA synchrotron in Basovizza (Trieste) and at the Deutsches Elektronen Synchrotron (DESY) in Hamburg. The data were collected at 100 K using 20% glycerol as cryoprotectant. Intensities were integrated with DENZO and scaled and merged with SCALEPACK (17). The data scaling indicates that the iron-loaded Dps crystals are orthorhombic $P2_12_12$ with unit cell dimensions of $a = 134.41$, $b = 139.65$, $c = 118.11$, as the crystals of native Dps. The structure of the iron-containing protein was refined using REFMAC (18). The $2F_o - F_c$ and $F_o - F_c$ maps were calculated for three different data sets using the program XTALVIEW (19).

Polarized Single Crystal Absorption Microspectrophotometry—Polarized single crystal absorption spectra have been obtained as described previously (20). The selected crystal was placed in a flow cell with quartz windows. When desired, the mother liquor was replaced by a medium of similar composition, containing a specific reagent. Spectra were collected using a Zeiss MPM800 microspectrophotometer. Absorption of the incident plane polarized light was recorded between 700 and 300 nm with a beam directed normal to a crystal face and the electric vector oriented in two perpendicular directions P1 and P2, each one representing an extinction direction of the crystal (20). Because of the irregular shape of the Dps crystals, it was not possible to identify the observed face nor the particular crystal axis along which spectra were collected. In the case of orthorhombic crystals, the *a*, *b*, and *c* axes coincide with the principal optical directions, along which absorption of polarized light obeys the Lambert and Beer law.

Kinetics of Iron Release in Crystals and in Solution—Sodium dithionite was used as reducing agent. Stock solutions of sodium dithionite (0.1 M) were prepared in 20 mM Tris-HCl, pH = 7.8, 200 mM NaCl, under purified nitrogen gas.

In the solution experiments, aliquots of 0.1 M sodium dithionite were added to 1 μM Dps containing 4 mM α-α′-bipyridyl in 20 mM Tris-HCl, pH = 7.8, by means of a gas tight syringe. The time course of reaction was monitored using a Hewlett-Packard Diode Array Spectrophotometer, equipped with a thermostatted cell maintained at 25 °C, and specifically followed at 520 nm, the wavelength corresponding to the absorption maximum of the Fe(II)-bipyridyl complex.

The kinetics of iron release within crystals was followed by monitoring the absorption decrease in the 450–300 nm region. The iron-loaded Dps crystals were stabilized by a solution of 0.1 M Tris-HCl, pH = 7.8, 1.4–1.7 M sodium formiate, and 9–12% PEG 8000 and placed in a flow cell. Iron release was induced by replacing the initial medium with a similar one containing 3 or 10 mM sodium dithionite.

The data were fitted using the program MATLAB (The Math Works Inc., Natick, MA).

[1] The abbreviation used is: PEG, polyethylene glycol.

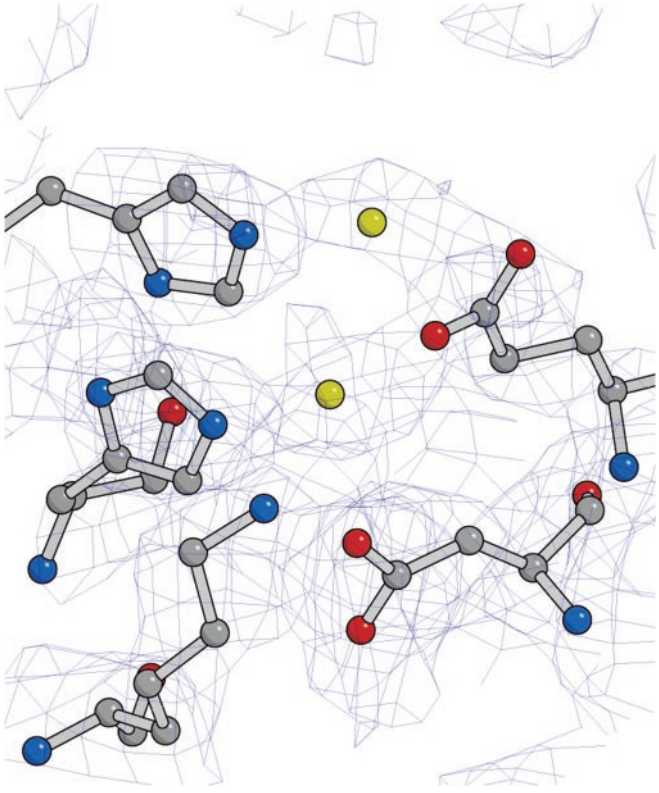

FIG. 1. **Electron density map of the ferroxidase site in *E. coli* Dps.** The proposed iron coordinating is indicated: Asp^{78} and Glu^{82} on one subunit (corresponding to Asp^{58} and Glu^{62} in *Listeria* ferritin), His^{51} and His^{63} (corresponding to His^{31} and His^{43} in *Listeria* ferritin) and Lys^{48} on the 2-fold symmetry related subunit. Lys^{48} is a Pb ligand in the *E. coli* Dps structure of Grant *et al.* (11); it forms a salt bridge with Asp^{78}. In the figure, two density peaks assigned to water molecules (in *yellow*) are also shown. The picture was prepared with the program BOBSCRIPT.

RESULTS

Structural Features of the Ferroxidase Center—The crystals of iron-loaded *E. coli* Dps are orthorhombic, similarly to the crystals of the native protein and its isomorphous derivative with Pb, studied by Grant *et al.* (10). At the interface of 2-fold symmetry related subunits, in the position corresponding to the ferroxidase center in *Listeria* ferritin, the $2F_o - F_c$ and $F_o - F_c$ maps show two distinct electron density peaks with an intensity higher than 3 σ (Fig. 1). The peaks can be assigned to water molecules forming strong hydrogen bonds with His^{51} and His^{63} from one subunit and Glu^{82} from the symmetry-related one. In the Dps crystals studied by Grant *et al.* (10), these amino acids provide the Pb ligands together with Lys^{48} and Asp67 from one subunit and Asp^{78} from the other. Lys^{48} forms a salt bridge with Asp^{78} (Nz-OD1 = 2.87 Å), which is in the position occupied by Asp^{58}, one of the iron ligands, in *Listeria* ferritin. It may be recalled that, in the crystal structure of *Listeria* ferritin, the ferroxidase center contains one iron ion and a water molecule, which is thought to replace the second iron ion, since a bimetallic intermediate is formed during the ferroxidation reaction (21).

Polarized Absorption Spectra—The solution spectra of iron-loaded Dps are characterized by an increasing absorption in the range between 400 and 300 nm due to the iron hydroxide stored within the protein cavity (Fig. 2). This feature is common to all ferritins (22).

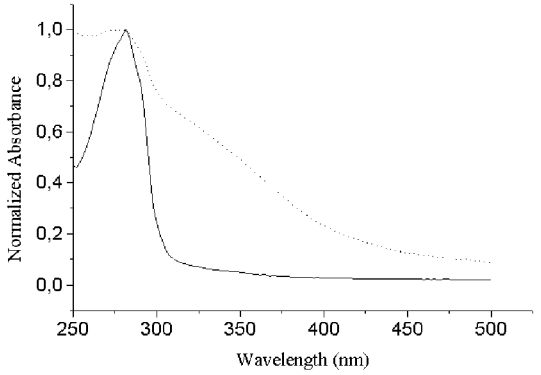

FIG. 2. **Absorption spectrum of soluble Dps in the iron-free and iron bound forms.** Iron-free (*dotted line*) and iron bound (*solid line*) protein in 30 mM Tris-HCl, pH = 7.8.

The polarized absorption spectra collected along P1 and P2 differ in shape and intensity (Fig. 3*A*). In the P2 direction the absorption spectrum is more intense but nearly featureless, whereas in the P1 direction it exhibits a weak absorption band in the 370 nm region, clearly observed in the difference spectrum (Fig. 3*C*). Based on the absorption spectrum of $[FeO_4]$ in iron-doped orthoclase feldspar, which displays a band with a maximum at 377 nm assigned to the d-d spin forbidden transition $^6A_1 \rightarrow {}^4A_1$, ^4E (23), this band may be assigned to Fe(III) tetracoordinated to oxygen atoms.

Treatment of the crystal with sodium dithionite causes a decrease of the crystal absorbance in both the P1 and P2 directions of about 45% (Fig. 3, *B* and *C*). Thus, dithionite causes iron reduction/release as in classical ferritins. It is noteworthy that, despite the large excess of dithionite, the absorption spectrum is not abolished. At the end of the experiment the crystal was washed with a solution of mother liquor without dithionite. There was no recovery of the signal, an indication of iron release in the medium.

Kinetics of Iron Reduction/Release in the Crystal and in Solution—To monitor the time course of iron reduction/release in Dps crystals, polarized absorption spectra along P1 were measured every 2 min after addition of dithionite in large excess. Spectral changes along this principal optical direction measure time-dependent changes in the concentration of the absorbing species. Fig. 4 shows that the decrease of the crystal absorbance at 372 nm as a function of time can be fitted to a mono-exponential curve and that the corresponding rate constant is $6.7 \times 10^{-4}\ s^{-1}$. This low rate is not limited by diffusion of dithionite through the crystal channels.

The time course of iron reduction/release by dithionite from soluble iron-loaded Dps at the same pH of 7.8 is shown in Fig. 5*A*. In these experiments iron release was followed at 520 nm, where formation of the complex between Fe(II) and α-α′-bipyridyl is monitored. The time course is biphasic with kinetic constants of $4.7 \times 10^{-2}\ s^{-1}$ and $1.2 \times 10^{-3}\ s^{-1}$ when dithionite is 5 mM. Fig. 5*A* shows that the fast phase accounts for 70% of the total absorbance change. A 2-fold variation of the bipyridyl concentration does not change the observed rates, indicating that formation of the Fe(II)-bipyridyl complex is rapid compared with the iron reduction/release process. Fig. 6 shows that the two kinetic constants depend similarly on dithionite concentration and that the dependence is not linear. It should be mentioned that parallel experiments in which iron reduction was assessed by following the decrease in absorbance at 380 nm yield the same results (data not shown).

The dependence of the reaction on pH was also studied. A decrease of pH to 6.5 results in the increase in the rate of both kinetic phases (Fig. 5*B*). The rate constants correspond to

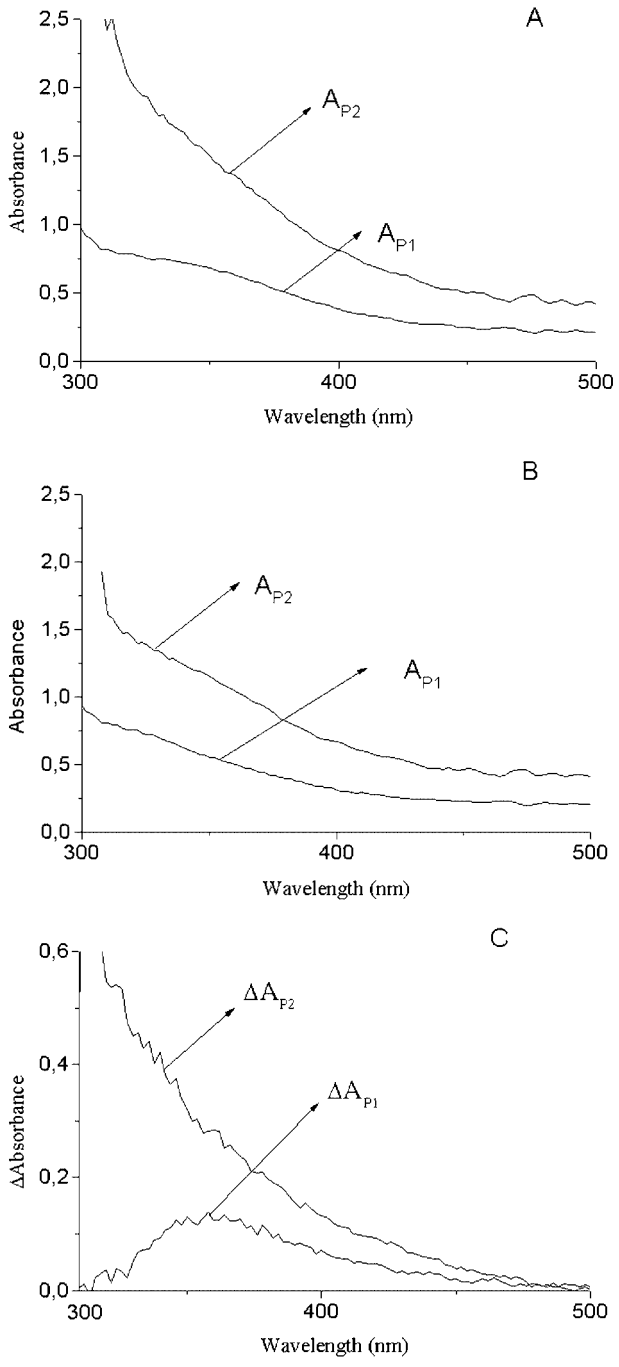

FIG. 3. **Polarized absorption spectra of a Dps crystal in the iron-bound (*A*) and dithionite-reduced form (*B*) and difference spectra A-B (*C*).** The electric field was oriented in two perpendicular directions (P1, P2). Conditions: 0.1 M Tris-HCl, pH = 7.8, 1.4–1.7 M sodium formiate, and 9–12% PEG 8000. In *B* the spectra were recorded 1 h after reduction with 10 mM sodium dithionite.

$14.2 \times 10^{-2}\ s^{-1}$ and $4.6 \times 10^{-3}\ s^{-1}$, respectively, at the dithionite concentration (5 mM) used for the experiment reported in *panel A*.

DISCUSSION

The present experiments contribute to define the ferritin-like properties of *E. coli* Dps, the prototype of the family. *E. coli* Dps is shown to behave like canonical ferritins in that it forms inside the protein cavity a microcrystalline oxyhydroxide core, which can be mobilized upon reduction. In addition, the affinity of the ferroxidase site for Fe(III) is shown to differ in Dps

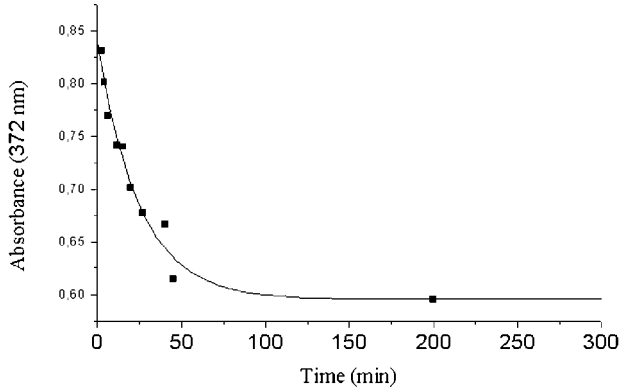

FIG. 4. **Time course of iron reduction/release by dithionite from iron-loaded Dps crystals.** The crystal was in 0.1 M Tris-HCl, pH = 7.8, sodium formiate 1.4–1.7 M, and 9–12% PEG 8000; sodium dithionite was 3 mM. The *curve* represents a fit of the data to a single exponential.

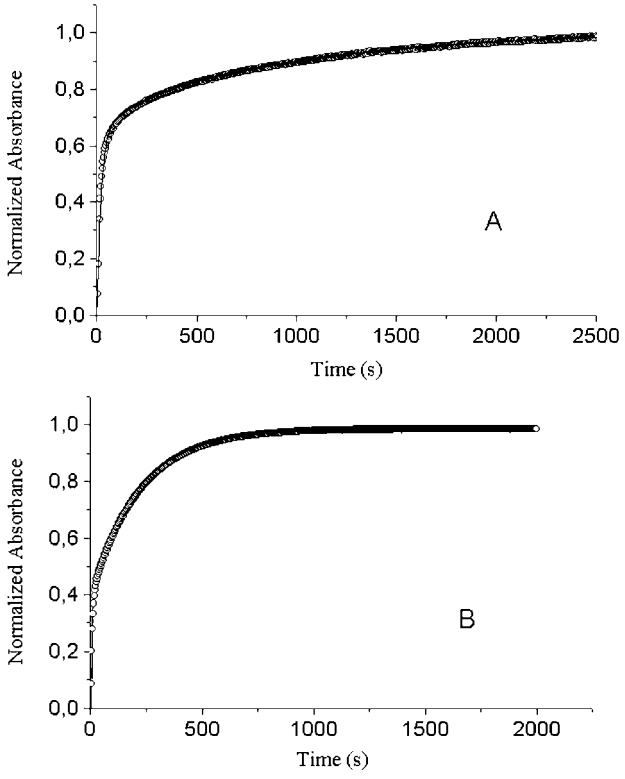

FIG. 5. **Kinetics of iron reduction/release by dithionite from iron-loaded soluble Dps in the presence of α-α′-bipyridyl.** Buffer: 30 mM Tris-HCl, pH = 7.8 (*A*) and 30 mM MOPS, pH = 6.5 (*B*). Formation of the Fe(II) α-α′-bipyridyl complex was followed at 520 nm.

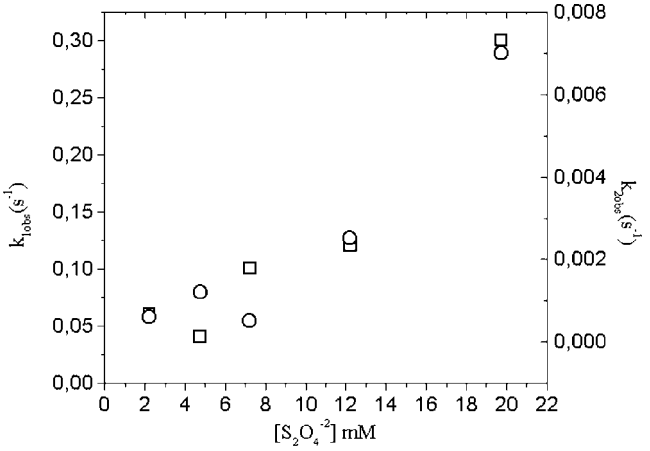

FIG. 6. **Plot of the rate constants for iron reduction/release from iron-loaded soluble Dps determined in Fig. 5 *versus* dithionite concentration.**

relative to *Listeria* ferritin where the redox center has the same unusual intersubunit location and most of the iron ligands in common.

All the investigations on the iron oxidation/incorporation properties of Dps proteins stem from the recognition that these proteins contain the *L. innocua* ferritin ferroxidase site as part of the so-called DNA-binding signature, the family characteristic (24). In *E. coli* Dps, the iron oxidation and hydrolysis reactions lead to incorporation inside the protein shell of about 400 iron ions with an overall mechanism that resembles closely that of *Listeria* ferritin (21). However, there is a distinctive difference between the two proteins related to the clearance from the original binding site of the two metal ions that participate in the redox reaction. In fact, Fig. 1 shows that in iron-loaded Dps crystals the ferroxidase center is occupied by two water molecules and not by the metal, in contrast with *L. innocua* crystals where one iron ion remains bound tightly to the site even after treatment with sodium dithionite (9). In turn, the absence of bound Fe(III) at the ferroxidase site of *E. coli* Dps crystals is in accordance with the observation that, in soluble Dps, the absorbance maximum at 297 nm attributed to this species decreases after a few hours to about 70%, due to movement of iron to the internal cavity (11). The relatively low affinity for Fe(III) in *E. coli* Dps may be ascribed to the presence of a salt bridge between Lys^{48} (His^{28} in *Listeria* ferritin) and Asp^{78} (Nz-OD1 = 2.87 Å), which is one of the metal ligands in the isomorphous derivative with Pb (10) and corresponds to one of the iron ligands in *Listeria* ferritin (Asp^{58}). This salt bridge limits the flexibility of the amino acid side chain and thereby decreases its coordination capacity. Therefore in Dps, despite the striking similarity with *Listeria* ferritin ferroxidase centers, both iron ions leave the bimetallic ferroxidase site to reach the internal cavity.

Two characteristic features of the ferritin oxyhydroxide iron core are its microcrystalline structure and its reductive mobilization. To establish whether the iron incorporated inside the Dps cavity shares these features, experiments have been performed both in solution and on single crystals. The polarized absorption spectra of crystals provide information on: (i) the presence of absorbing species and their degree of order and (ii) the fine structure of such species. In the case of the iron core here described, one can establish the coordination symmetry of the metal in the core, since Fe(III) coordinated tetrahedrally with oxygen has a typical absorption band at around 380 nm, whereas Fe(III) coordinated octahedrally with oxygen has absorption bands in the near infrared region and in the visible region at 550 nm and 407 nm, all ascribable to d-d transitions (23). The results reported in Fig. 3 demonstrate unambiguously that the *E. coli* Dps iron core is ordered and that the metal is tetrahedrally coordinated with oxygen, given the presence of a distinct band at about 372 nm and the absence of bands at higher wavelengths. It may be envisaged that Fe(III) and oxygen atoms form a crystal with tetrahedral symmetry where the tetrahedron center is occupied by iron ions and the vertices by oxygen. The result is of interest in light of the fact that the available literature data, obtained with other spectroscopic techniques, do not yield clear-cut answers with respect to the iron coordination geometry in ferritins. Thus, Mössbauer spectra measured on horse spleen ferritin and model compounds are indicative of a octahedral coordination (8). In contrast,

TABLE I
Rate constants for iron reduction/release by dithionite from E. coli Dps and ferritins
The rate constants refer to a dithionite concentration around 5 mM.

	k_1 (s^{-1})	k_2	Taken from
Soluble Dps at pH 6.5 (from $A_{520\ nm}$)	14.2×10^{-2}	4.6×10^{-3}	Present work
Soluble Dps at pH 7.8			
From $A_{520\ nm}$	4.7×10^{-2}	12.0×10^{-4}	Present work
From $A_{380\ nm}$	6.8×10^{-2}	7.8×10^{-4}	Present work
Dps crystals at pH 7.8		6.7×10^{-4}	Present work
Horse spleen ferritin at pH 8.0		3.3×10^{-4}	Ref. 26
A. vinelandii bacterioferritin at pH 7.0	2.6×10^{-2}	1.8×10^{-3}	Ref. 28
Pig spleen ferritin at pH 9.0	2.3×10^{-3}	1.5×10^{-3}	Ref. 29

x-ray scattering data on model compounds (25) indicate that iron coordination is tetrahedral.

The iron reduction/release reaction measured on Dps crystals and in solution shows that the microcrystalline iron core is readily mobilizable after reduction as is the case for all known ferritins. The choice of dithionite as a reducing agent has been dictated by two considerations: it can diffuse easily through the crystal liquid channels, and it has been used for a number of ferritins (26–29). The reduction/release process, despite its complexity as it involves several steps including diffusion of dithionite inside the protein, electron transfer from dithionite to Fe(III), and protonation of hydroxide ions, appears to be a biphasic process when measured in solution with the fast phase taking place in a few seconds at neutral pH and millimolar dithionite concentrations (Fig. 5). It is not surprising therefore that this phase cannot be followed on single crystals where only one slow process is observed (Fig. 4). The slow reaction has comparable rates in crystalline and soluble Dps and, in the latter case, both in the absence and in the presence of the Fe(II) chelator α-α'-bipyridyl. It follows that both dithionite diffusion through the crystal liquid channels and binding of Fe(II) to the chelating agent are not rate-limiting. Upon decrease of pH from 7.8 to 6.5 the rate of iron reduction in solution increases about 2-fold as shown in Fig. 5 and reported for all known ferritins (26–29). It is of interest to compare the present findings on Dps with the literature data involving classical ferritins and dithionite (Table I). Two kinetic phases have been observed in pig spleen ferritin, a fast, first order reaction for iron release from the surface of the core and a slower zero order reaction involving iron inside the core (29). In *Azotobacter vinelandii* heme-containing ferritin a similar biphasic reduction process takes place, albeit with different characteristics, since both phases depend on dithionite concentration in a complex manner. They have been ascribed to reduction of two different populations of iron atoms, those in the core and those attached to the interior of the shell or associated to the heme groups (28). Similarly, the two phases observed in the kinetics of iron release from soluble Dps may be taken to reflect the presence of two distinct iron populations.

In conclusion, the capacity of *E. coli* Dps to direct iron deposition toward formation of a microcrystalline iron core and the behavior of the core itself attendant reduction furnish additional evidence for the ferritin-like function of this class of proteins. It remains to be established how these properties act in cooperation, on the one hand, with iron uptake to achieve iron homeostasis and, on the other hand, with physical association to DNA to protect it effectively against oxidative damage.

Acknowledgment—We thank Dr. Laura Giangiacomo for carrying out the ultracentrifuge control experiments.

REFERENCES

1. Ford, G. C., Harrison, P. H., Rice, D. W., Smith, J. M. A., Treffry, A., White, J. L., Yariv, J. (1984) *Philos. Trans. R. Soc. Lond.* **304,** 551–565
2. Boyd, D., Vecoli, C., Belcher, D. M., Jain, S. K., and Drysale, J. W. (1985) *J. Biol. Chem.* **260,** 11755–11761
3. Bozzi, M., Mignogna, G., Stefanini, S., Barra, D., Longhi, C., Valenti, P., and Chiancone, E. (1997) *J. Biol. Chem.* **272,** 3259–3265
4. Clegg, G. A., Fitton, J. E., Harrison, P. M., and Treffry, A. (1980) *Prog. Biophys. Mol. Biol.* **36,** 56–86
5. Haggis, G. H. (1965) *J. Mol. Biol.* **14,** 598–602
6. Harrison, P. M., Fischbach, F. A., Hoy, T. G., and Haggis, G. H. (1967) *Nature* **216,** 1188–1190
7. Massover, W. H., and Cowley, J. M. (1973) *Proc. Natl. Acad. Sci.* U. S. A. **36,** 3847–3851
8. Harrison, P. M., Lilley, T. H. (1989) in *Iron Carriers and Iron Proteins* (Loehr, T., ed) pp. 123–238, VCH Publishers, Inc., New York
9. Ilari, A., Stefanini, S., Chiancone, E., Tsernoglou, D. (2000) *Nat. Struct. Biol.* **7,** 38–43
10. Grant, R. A., Filman, D. J., Finkel, S. E., Kolter, R., and Hogle, J. M. (1998) *Nat. Struct. Biol.* **5,** 294–303
11. Zhao, G., Ceci, P., Ilari, A., Giangiacomo, L., Laue, T. M., Chiancone, E., and Chasteen, N. D. (2002) *J. Biol. Chem.* **277,** 27689–27696
12. Tonello, F., Dundon, W. G., Satin, B., Molinari, M., Tognon, G., Grandi, G., Del Giudice, G., Rappuoli, R., Montecucco, C. (1999) *Mol. Microbiol.* **34,** 238–246
13. Mozzarelli, A., and Rossi, G. L. (1996) *Annu. Rev. Biophys. Biomol. Struct.* **25,** 343–365
14. Almiron, M., Link, A. J., Furlong, D., and Kolter, R. (1992) *Genes Dev.* **6,** 2646–2654
15. Stefanini, S., Cavallo, S., Montagnini, B., and Chiancone, E. (1999) *Biochem. J.* **349,** 783–786
16. Bothwell, T. H., and Mallet, B. (1955) *Biochem. J.* **59,** 599–602
17. Otwinowski, Z., and Minor, W. (1997) *Methods Enzymol.* **276,** 307–326
18. Murshudov, G. N., Lebedev, A., Vagin, A. A., Wilson, K. S., and Dodson, E. J. (1999) *Acta Crystallogr.* Sect. *D Biol. Crystallogr.* **55,** 247–255
19. McRee, D. E. (1993) *Practical Protein Crystallography*, pp. 365–374, Academic Press, San Diego, CA
20. Rivetti, C., Mozzarelli, A., Rossi, G. L., Henry, E. R., and Eaton, W. A. (1993) *Biochemistry* **32,** 2888–2906
21. Yang, X., Chiancone, E., Stefanini, S., Ilari, A., and Chasteen, N. D. (2000) *Biochem. J.* **349,** 783–786
22. Treffry, A., and Harrison, P. M. (1984) *J. Inorg. Biochem.* **21,** 9–20
23. Webb, J., and Gray, H. B. (1974) *Biochim. Biophys. Acta* **351,** 224–229
24. Halligan, B. D. (1993) *Nucleic Acids Res.* **21,** 5520–5521
25. Towe, K., M., and Bradley, W., F. (1967) *J. Colloid Interface Sci.* **24,** 384–390
26. Stefanini, S., Chiancone, E., Vecchini, P., and Antonini, E. (1975) in *Proteins of Iron Storage and Transport in Biochemistry and Medicine* (Crichton, R. R., ed) pp. 295–302, North Holland Publishing Company, Amsterdam
27. Funk, F., Lenders, J. P., Crichton, R. R., and Schneider, W. (1985) *Eur. J. Biochem.* **152,** 167–172
28. Richards, T. D., Pitts, K. R., Watt, G. D. (1996) *J. Inorg. Biochem.* **61,** 1–13
29. Huang, Q., Lin, Q. M., Kong, B., Zeng, R. Y., Qiao, Y. H., Chen, H., Zhang, F. Z., and Xu, L. S. (1999) *J. Protein Chem.* **18,** 497–504

Iron Incorporation into *Escherichia coli* Dps Gives Rise to a Ferritin-like Microcrystalline Core

Andrea Ilari, Pierpaolo Ceci, Davide Ferrari, Gian Luigi Rossi and Emilia Chiancone

J. Biol. Chem. 2002, 277:37619-37623.
doi: 10.1074/jbc.M206186200 originally published online August 5, 2002
